Replaceable neurons and neurodegenerative disease share depressed *UCHL1* levels

Anthony J. Lombardino*, Xiao-Ching Li†, Moritz Hertel†, and Fernando Nottebohm

Laboratory of Animal Behavior, The Rockefeller University, Box 137, 1230 York Avenue, New York, NY 10021

Contributed by Fernando Nottebohm, April 20, 2005

Might there be systematic differences in gene expression between neurons that undergo spontaneous replacement in the adult brain and those that do not? We first explored this possibility in the high vocal center (HVC) of male zebra finches by using a combination of neuronal tracers, laser capture microdissection, and RNA profiling. HVC has two kinds of projection neurons, one of which continues to be produced and replaced in adulthood. HVC neurons of the replaceable kind showed a consistent and robust underexpression of the deubiquitination gene ubiquitin carboxyl-terminal hydrolase (*UCHL1*) that is involved with protein degradation. Singing behavior, known to increase the survival of adult-born HVC neurons in birds, significantly up-regulated the levels of *UCHL1* in the replaceable neurons but not in their equally active nonreplaceable counterparts. We then looked in the mouse brain and found relatively low *UCHL1* expression in granule neurons of the hippocampus and olfactory bulb, two well characterized types of replaceable neurons in mammals. UCHL1 dysfunction has been associated with neurodegeneration in Parkinson's, Alzheimer's, and Huntington's disease patients. In all these instances, reduced UCHL1 function may jeopardize the survival of CNS neurons.

adult neurogenesis | gene expression | laser capture microdissection | neurodegeneration

Spontaneous neuronal replacement occurs in a regulated manner in specific regions of the adult vertebrate brain (1–6). In these regions new neurons replace older ones of the same kind that have spontaneously died. The new neurons are born in the ventricular zone lining the lateral ventricles of birds (7) and in the subventricular zone of the lateral ventricle and the hippocampal subgranular zone of mammals (8), from where they migrate to their eventual destination (9, 10). Once the new neurons stop migrating, they differentiate and connect to existing circuits (11, 12). Neurons added to the adult brain send projections to local or distant targets, depending on the type of neuron that the new cell becomes. Typically there is an overproduction of new neurons; the extent of initial culling (13) and the duration of subsequent survival are influenced by circuit use (14–16). Many of these aspects of production, migration, connection, and survival of neurons born in the adult brain were first established in the song system of birds, which offers rich material for studying adult neurogenesis and neuronal replacement in the context of a learned behavior (1).

An outstanding question about neuronal replacement in adult brain concerns the properties of neurons that are spontaneously replaced after they have taken up residence in a functioning circuit. This category of "replaceable neurons" includes premotor neurons in the song system of birds (2), short-range projection neurons in the dentate gyrus (DG) of the mammalian hippocampus (17), and granule cell interneurons in the mammalian olfactory bulb (6). Are these replaceable neurons similar to comparable classes of neurons that are not normally replaced in adult life? Or are there features shared by all replaceable neurons that are related to their peculiarly transient status? Of course, all neurons in either class need not be alike. For example, there is evidence for heterogeneity within a specific population of replaceable cells, perhaps based on exact cellular age (18, 19). We first approached these questions by directly comparing the genes expressed in replaceable and nonreplaceable projection neurons from the high vocal center (HVC) of the zebra finch (*Taeniopygia guttata*). Our results show that in zebra finches and mice, a gene implicated in protein turnover, ubiquitin carboxyl-terminal hydrolase (*UCHL1*), is expressed at consistently lower average levels in replaceable neurons as compared with nonreplaceable neurons. We show that, in the avian case, the level of expression of this gene increases when the neurons are activated by behavior (singing), a stimulus that also increases their survival (20). Because deficiencies in UCHL1 expression have been associated with neurodegenerative disease, it could be that the basic biology of spontaneous neuronal replacement will shed light on the etiology of neural degeneration.

Materials and Methods

Subjects, Surgery, and Behavior. This study used 19 adult male zebra finches aged 6 months to 3 years and 12 adult mice aged 3–8 months (Swiss–Webster or Black 6 background) raised at The Rockefeller University's animal facilities. The care of the animals used in our experiments was in accordance with the standards set by the American Association of Laboratory Animal Care and The Rockefeller University Animal Use and Care Committee. Birds were anesthetized (25 mg/kg ketamine and 60 mg/kg xylazine) and injected in each hemisphere with 1% cholera toxin B (40 nl per site) conjugated to Alexa Fluor dyes (Molecular Probes). These injections were targeted to robust nucleus of arcopallium (RA) and Area X and, after transport, allowed visualization of HVC's projection neurons in two different colors (Fig. 1*a*). Henceforth, these neurons will be referred to as HVC-RA and HVC-X neurons. HVC-RA neurons are smaller and more numerous than HVC-X neurons, and the two cell classes do not overlap (21), as shown in Fig. 1*b*. Only the RA-projecting neurons are replaced in adult birds (22), even when neuron death is induced (3). No differences were seen between presurgery and postsurgery song recordings (data not shown), indicating that neuron function was unaffected. Birds and mice were killed by decapitation, and their brains were frozen, sectioned on a cryostat at 10 μm, and prepared for laser capture microdissection as described below.

Laser Capture Microdissection of Identified Populations of Projection Neurons, RNA Procurement, and Amplification. Cell bodies from backfilled HVC-RA and HVC-X neurons, each with their own expressed RNAs, were identified by fluorescence in frozen tissue sections and microdissected using a laser capture microscope (Pixcell IIe, Arcturus Bioscience, Mountain View, CA) (Fig. 1 *b* and *c*). We microdissected 2,000 HVC-RA neurons and 1,500 HVC-X neurons per bird from all regions of both HVCs,

Abbreviations: UCHL1, ubiquitin carboxyl-terminal hydrolase; RA, robust nucleus of arcopallium; HVC, high vocal center; DG, dentate gyrus; aRNA, amplified RNA; q-PCR, quantitative PCR.

Data deposition: The sequence reported in this paper has been deposited in the GenBank database (accession no. DQ005532).

*To whom correspondence should be addressed. E-mail: lombara@mail.rockefeller.edu.

†X.-C.L. and M.H. contributed equally to this work.

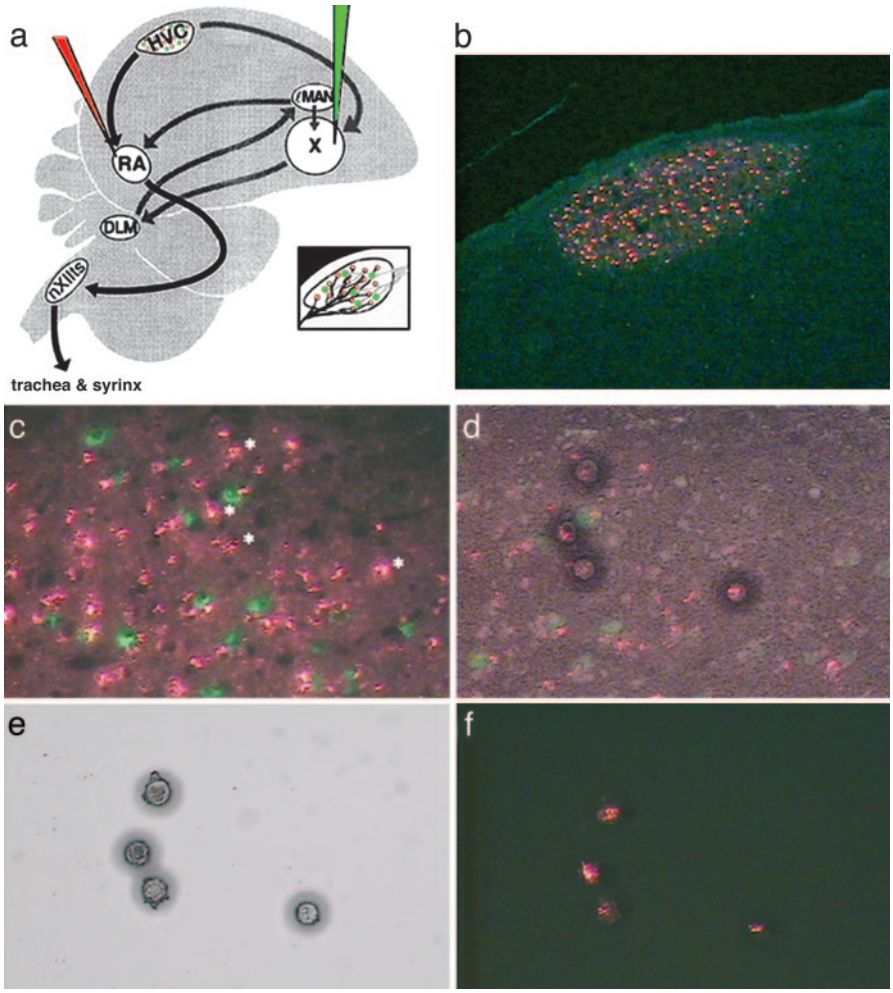

Fig. 1. Labeling and microdissection of long-range projection neurons in nucleus HVC. (*a*) Diagram of the principal nuclei of the song system, including HVC; the micropipettes were used to backfill HVC projection neurons from RA (red) and X (green). (*b*) Low-magnification (×20) micrograph of HVC shows the projection neurons backfilled from RA and X; the more numerous RA-projecting neurons give HVC a reddish appearance. (*c–f*) Backfilled neurons were selected for microdissection (note white asterisks near red RA-projecting neurons) (*c*), the overlying plastic was melted into the cells (*d*), and the laser capture microdissection cap was removed, revealing captured cell material (*e*) bearing tracer fluorescence (*f*).

resulting in similar amounts of RNA for each cell class. Confirmation that cellular material from the soma was removed from the sections came from seeing the retained fluorescent tracer in the captured material (Fig. 1 *d–f*). For the mouse hippocampus, 1,000 neurons identified by histological staining (HistoGene, Arcturus Bioscience) and position were captured one-by-one from each of seven mice. Neurons from each of the following subregions were captured: CA1/CA2 (taken together), CA3, and DG. For mouse olfactory bulb, 500 HistoGene-stained neurons were captured from the mitral cell layer or granule cell layer from each of four mice. Although backfilling was a necessary step for cell identification in HVC, this was not the case for the cells of hippocampus and olfactory bulb, which segregate by layers. RNA was column-purified (PicoPure, Arcturus Bioscience), treated with DNase (Qiagen, Valencia, CA), and amplified through two rounds with the RiboAmp HS kit (Arcturus Bioscience), which is based on the linear T7 amplification technique developed by Eberwine and colleagues (23). The yield of purified antisense amplified RNA (aRNA) was ≈90 μg from each neuron type per bird, 400–1,000 bp in length, and was measured in triplicate by using a bioanalyzer (Agilent Technologies, Palo Alta, CA). A mean of these measures was taken to calculate the input aRNA for the microarray and quantitative PCR (q-PCR) assays. The linearity of the amplification process was confirmed (see Fig. 8, which is published as supporting information on the PNAS web site).

cDNA Microarray Construction and Hybridizations. Total brain mRNA from zebra finches of different developmental stages (embryonic, juvenile, and adult) was used to make cDNA libraries. The cDNA libraries were oligo(dT) primed and cloned into the EcoRI and NotI sites of pBluescript plasmid vector. Randomly picked clones were sequenced from the 3′ end, yielding 700–800 nucleotides of readable sequence. Sequence analysis was performed with the MAGPIE system, a high-throughput clone analysis and annotation program. Our microarray consisted of a random selection of 768 unique clones printed on a glass slide. Equal amounts of the two-round aRNA from each projection neuron type were reverse transcribed in the presence of Cy3- or Cy5-coupled UTP (Amersham Pharmacia), respectively, in a direct labeling reaction. Two-color cDNA microarrays were hybridized with this labeled cDNA, with each bird's RA-projecting cDNA compared with its own X-projecting cDNA (i.e., within-bird comparisons). We ran duplicates and duplicate fluor-flips for a total of four microarray slides per bird, with each slide containing three replicate microarrays. Thus, for

data analysis each spot was represented 12 times for each bird; because we pooled 14 birds' worth of comparisons, this gave 168 total representations of each spot. After hybridization, intensity readings at each wavelength were imported to the software package GENETRAFFIC DUO (Iobion Informatics, La Jolla, CA) for normalization (LOWESS subgrid method) and quantitative analysis of differential expression.

Sequencing and Gene Identification. Sequencing of the finch *UCHL1* clone (GenBank accession no. DQ005532) was performed from both sides. To obtain the full-length clone, the two overlapping sequences were joined and aligned to human (GenBank accession no. NM_004181) and murine (GenBank accession no. AF172334) sequences. Identity to the human and murine sequences was 77% and 74%, respectively. Amino acid identity was 74% to human and 72% to mouse. The *E* value for the human DNA sequence comparison, representing the probability that these sequences match by chance, is 2×10^{-104}.

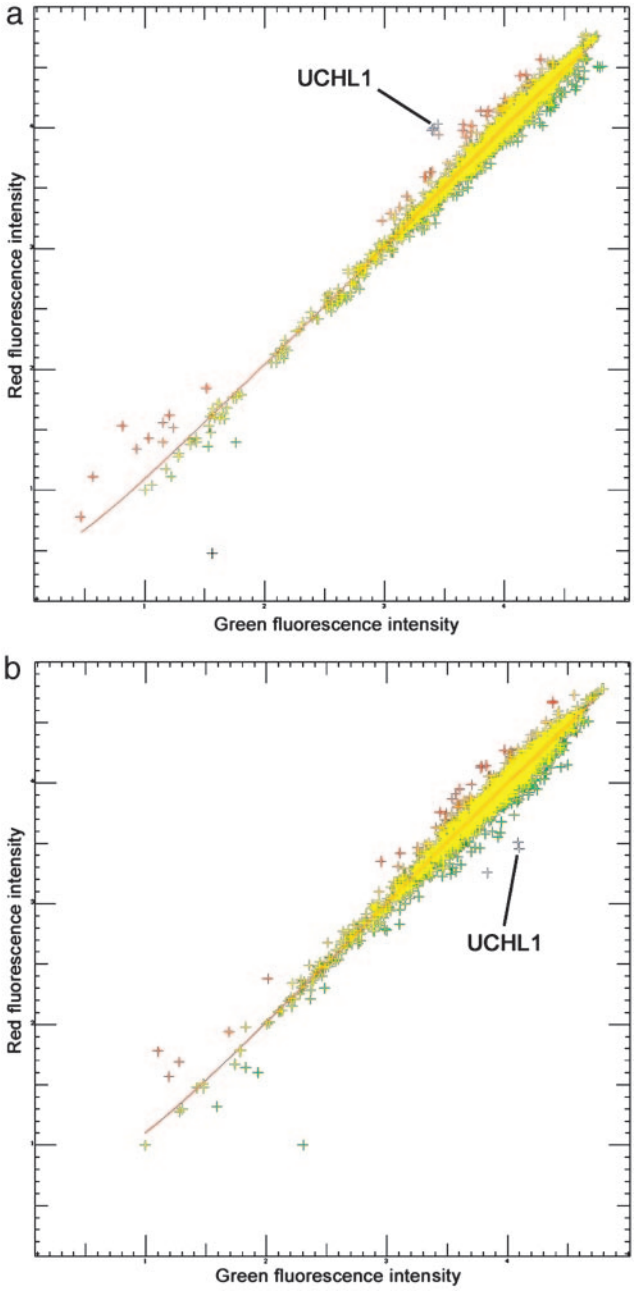

Fig. 2. Plots of fluorescence intensity at each of the scanned wavelengths for two microarray slides. (*a*) The cDNA from the X-projecting cells was labeled red (Cy5), and that from the RA-projecting cells was labeled green (Cy3). (*b*) The labels in *a* are reversed. Each cross represents a spot on the array, with the 768-spot array having been printed in triplicate on each slide. Note that most spots show equal expression (yellow), whereas outliers are red or green. The spots for UCHL1 (in triplicate) are highlighted in gray.

q-PCR. Equal amounts of aRNA HVC-RA and HVC-X neurons ($n = 13$ birds) or of mouse hippocampal neurons ($n = 11$ mice) were reverse-transcribed (RETROscript kit, Ambion, Austin, TX). The cDNA was used in TaqMan q-PCR assays with primers and probes (Applied Biosystems) designed against zebra finch or mouse sequences using PRIMER EXPRESS software (Applied Biosystems). Reactions were run in triplicate in a total volume of 25 μl. Standard curves were constructed from serial dilutions of purified DNA (Sigma-Genosys) corresponding to the predicted amplicon; these were used to calculate absolute copy numbers of *UCHL1* in the amplified material, as described in ref. 24. Normalization of TaqMan data were to total RNA (24, 25). The efficiency of our TaqMan PCR reaction depended on the exact primer/probe combination used, making direct comparisons between species problematic. Student's *t* tests were used to assess the significance of differences between group means as indicated in the figure legends.

Cloning of Mouse *UCHL1* Full-Length Probe. Primers were designed against the full mouse coding sequence of *UCHL1* (accession no. AF172334). The sequence was amplified from mouse brain with oligo(dT) priming and reverse-transcribed into cDNA. The DNA was gel-purified and cloned into plasmid pCR II-TOPO vector (Invitrogen). Clone identity was confirmed by sequencing, and an antisense probe was designed by HindIII digestion and transcription from the T7 promoter with [^{33}P]UTP.

***In Situ* Hybridization.** Fresh frozen sections 6–12 μm thick were fixed in 4% cold fresh formaldehyde and hybridized with 10^6 cpm of [^{33}P]UTP-labeled antisense probe, as per standard *in situ* procedures, including prehybridization acetylation of the sections and a posthybridization RNase digest. After dipping in x-ray film emulsion (Kodak), the sections were exposed for 2.5–4.0 weeks and developed. The density of silver grains over each cell type was assessed under darkfield and brightfield conditions. These results were used to confirm visually the microarray and TaqMan quantification. Because the autoradiography results agreed with the other two analyses and were obvious by direct examination, we did not count silver grains.

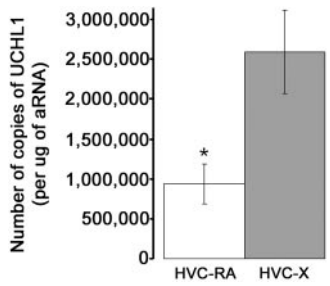

Fig. 3. Relative expression levels of *UCHL1* in zebra finch HVC as determined by q-PCR. Shown are average levels of *UCHL1* from HVC-RA and HVC-X neurons collected from all birds in the experiment, as assessed by TaqMan q-PCR. The difference is significant in an unpaired, two-tailed, unequal variance Student *t* test, with $P = 0.00007$. Error bars indicate SEM.

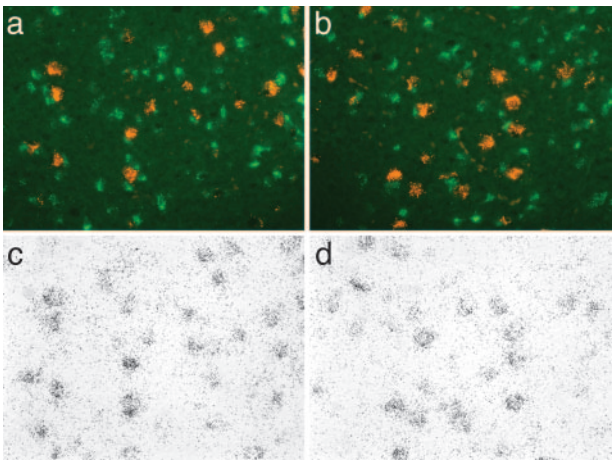

Fig. 4. Expression levels of *UCHL1* in zebra finch HVC projection neurons shown by *in situ* hybridization. (*a* and *b*) Backfilled HVC projection neurons from two birds, with RA-projecting neurons in green and X-projecting neurons in red. (*c* and *d*) As predicted, the largest clusters of exposed silver grains are found over the X-projecting neurons.

Results

Most spots in our microarray showed similar expression levels for the HVC-RA and HVC-X material, resulting in yellow coloration (Fig. 2), as might be expected for a within-subject comparison of two projection neuron subtypes from a common brain region. Our criterion for overexpression of a gene was that the cDNA for that gene had to be at least 2-fold more abundant in one cell type than in the other. In this manner, we hoped to highlight the extremes of differential gene expression. Across all replicates from all birds, 129,624 spots were hybridized in this experiment, and 1.8% reached our required level of overexpression. We selected for sequencing only those clones that met the "2-fold or higher" criterion in at least 50% of the 168 spots representing that gene over all replicate arrays for all birds. We did this to ensure that we would focus on the most robust and consistent expression differences over the replicate arrays. The present report is about the gene that most consistently met our overexpression criterion in the HVC-RA versus HVC-X comparison.

***UCHL1* Is Underexpressed in HVC's Replaceable Projection Neurons.** The clone on our microarray showing the most consistent differential expression was sequenced and identified as the zebra finch homolog of *UCHL1* (Fig. 2), a neuron-specific gene with a protein product thought to comprise 1–2% of soluble brain protein (26, 27). *UCHL1* was formerly identified as PGP9.5 and used as a universal marker for vertebrate neurons (28). On our microarrays, this gene was overexpressed in HVC-X neurons in 59% of its spots from birds of all adult age groups regardless of singing status. The average overexpression of this gene for all birds, as assessed by the microarrays, was 2.23-fold. TaqMan q-PCR amplification curves, generated from the same samples of aRNA described above, confirm the microarray results. For the within-bird comparison, the number of amplified copies of *UCHL1* was on average 2.39-fold higher in HVC-X neurons than HVC-RA neurons. Summed over all birds, the average overexpression in the HVC-X neurons was 2.76-fold greater than in the HVC-RA neurons (Fig. 3). Comparing each bird's q-PCR and microarray data gave a correlation coefficient of 0.86. *In situ* hybridization also confirmed the pattern of differential *UCHL1* expression, with numerous clusters of grains over X-projecting neurons and few if any over the RA-projecting neurons (Fig. 4). The high expression of *UCHL1* as determined by *in situ* hybridization in HVC-X neurons was comparable with that in other neurons outside of HVC (data not shown), as would be expected for a panneuronal marker with high evolutionary conservation (29). Although we set out to discover rare genes up-regulated in neurons turning over in adulthood, our array analysis led us to see the low expression of an abundant gene, *UCHL1*, in HVC-RA neurons as the noteworthy expression pattern.

Replaceable Neurons in Mice also Show Low Levels of *UCHL1*. HVC's projection neurons presumably differ along many dimensions; therefore, the differences we saw in *UCHL1* expression between RA- and X-projecting neurons could have resulted from variables other than the replaceability of the cells. To test the idea that depressed levels of *UCHL1* correlate with the replaceable nature of some neuronal types, we used *in situ* hybridization to assess *UCHL1* expression in the principal neurons known to undergo replacement in the brains of adult mice ($n = 10$). In the hippocampus (Fig. 5 *a–d*) and olfactory bulb (Fig. 5 *e–g*), there were markedly low levels of mouse *UCHL1* in layers known to contain replaceable neurons (30, 31), compared with adjacent layers where neurons are not normally replaced. In the hippocampus, the lowest *UCHL1* expression was seen in the granule cell layer of the DG, compared with the CA regions; in the olfactory bulb, the lowest expression was seen in the granule cell layer, compared with the mitral cell layer. To confirm the hippocampal expression pattern seen in the *in situ* hybridiza-

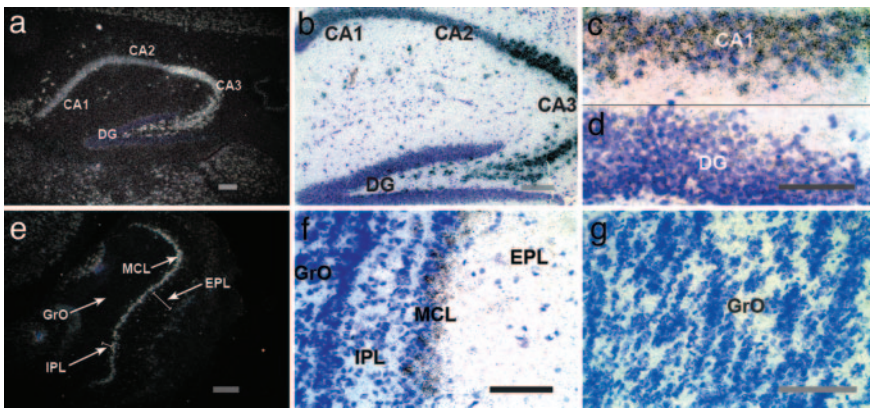

Fig. 5. Expression of *UCHL1* in adult mouse brain by *in situ* hybridization. (*a* and e) Darkfield sections show an overview of the two regions where new neurons are added to replace others that have died. (*a–d*) In the hippocampus, adult-born neurons are found in the DG, which shows very low *UCHL1* expression. (*c* and *d*) DG and CA1 cells, separated by a black line, are compared at higher magnification (×100). (*e–g*) In the olfactory bulb, new neurons are added to the granule cell layer (GrO) but not to the mitral cell layer (MCL). The granule cells of the DG and olfactory bulb show low levels of label compared with nearby CA neurons of hippocampus or mitral cells of the olfactory bulb. IPL, internal plexiform layers; EPL, external plexiform layers. (Scale bars, 100 μm.)

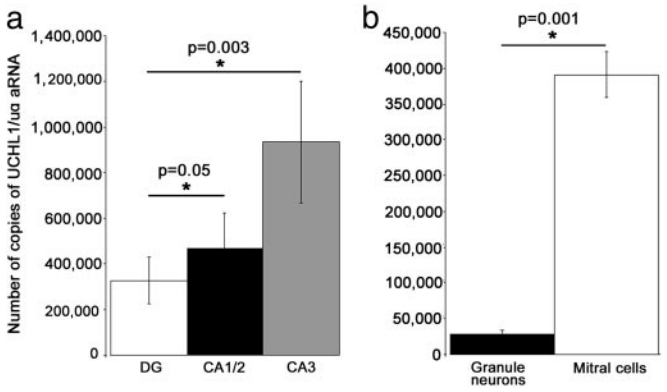

Fig. 6. *UCHL1* gene levels in mouse hippocampal and olfactory bulb subregions as determined by TaqMan q-PCR. (*a*) The absolute levels of *UCHL1* (normalized to total RNA) in the amplified material from CA1/CA2, CA3, and DG of the hippocampus, confirming the *in situ* results. The differences between regions indicated are significant in a paired, two-tailed Student *t* test at the indicated *P* level. Each bar represents the averages for 1,000 neurons of each type from each of seven mice. (*b*) The data from the olfactory bulb are shown. Each bar represents averages for 500 neurons of each type captured from each of four mice. Error bars indicate SEM.

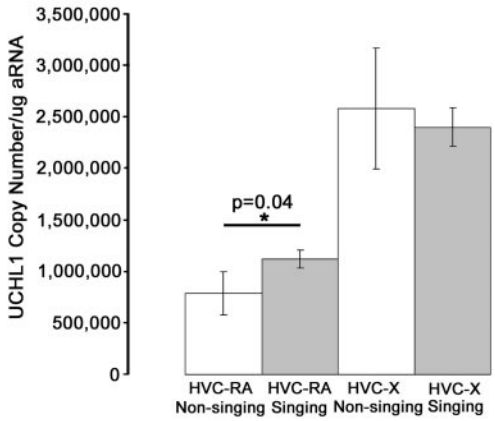

Fig. 7. Up-regulation of UCHL1 with singing. The significant increase in UCHL1 levels with singing is specific to HVC-RA neurons (unpaired, one-tailed, unequal variance Student's *t* test). Bars show the means and standard errors for birds that did not sing before being killed (white, $n = 7$) or sang to a female for 30 min (gray, $n = 5$).

tions, RNA was extracted from sets of 1,000 neurons laser captured from the following hippocampal regions: CA1 and CA2 taken together, CA3, and granule cells of the DG. Data from q-PCR assays for mouse *UCHL1* confirm the *in situ* hybridization results (Fig. 6). DG shows 43% less *UCHL1* expression than the CA1/CA2 regions, and 186% less than CA3 ($n = 7$ mice) (Fig. 6*a*). The olfactory bulb comparisons showed granule neurons to have 1,275% less *UCHL1* than the mitral cells ($n = 4$ mice, 500 neurons per region per animal) (Fig. 6*b*).

Up-Regulation of *UCHL1* in HVC-RA Neurons with Singing Behavior. A homolog of *UCHL3* can function as an immediate-early gene in *Aplysia* (32), and synthesis of *UCHL1* can be induced under toxic conditions (33). We had an indication that the levels of this gene might be regulated by singing in our birds because the fold-change microarray data showed a smaller difference between HVC's replaceable and nonreplaceable projection neurons in birds that had sung for 10 min and then were killed compared with nonsinging birds. In the song system, singing behavior is known to increase the survival of HVC neurons born in adulthood (14, 20), so we hypothesized that if levels of *UCHL1* are related to neuronal death or survival, they should increase with singing in HVC-RA neurons. We used our q-PCR assay to examine the levels of this gene in each of the two types of projection neuron in HVC in a second group of birds allowed to sing for a longer time than the first group: 30 min of song directed to a female at close range followed by 1 h during which the bird remained alone. Compared with birds that had not sung before being killed, these singers showed significantly elevated levels of *UCHL1* in their HVC-RA neurons but not in their HVC-X neurons (Fig. 7). The up-regulation of *UCHL1* expression in RA-projecting neurons averaged 43% and, thus, did not approach the much higher levels seen in HVC-X neurons. The singing-induced up-regulation of *UCHL1* expression cannot be explained by a simple increase in neuronal activity, because HVC-RA and HVC-X neurons go from a quiescent state to a similarly active state with singing (M. S. Fee, personal communication).[‡]

[‡]Kozhevnikov, A. A. & Fee, M. S. (2004) *Soc. Neurosci. Abstr.*, 786.6.

Discussion

We used expression profiling of specific types of songbird neurons to identify a gene that is underexpressed in a replaceable projection neuron compared with its expression in a nonreplaceable one; these two neurons occur side-by-side in the avian nucleus HVC. The results extend to similar comparisons between replaceable and nonreplaceable neurons in the adult mouse brain. We have also shown that in birds the expression of this gene increases with singing in the replaceable HVC neuron we studied but not in its nonreplaceable counterpart. Because singing also increases the life expectancy of HVC's replaceable neurons, rising levels of UCHL1 may be associated with a reduced risk of dying. Support for this association comes from deficiencies in UCHL1 expression found in neurodegenerative disorders, as discussed below.

Sampling of Neurons Undergoing Neurogenesis in Adulthood. Our use of laser capture microdissection and neuronal tracers gave us access to well defined populations of specific neurons, but the cells we sampled, particularly in the replaceable category, probably had a diversity of ages. Standard methods for birth-dating a cohort of neurons, such as labeling with tritiated thymidine or bromodeoxyuridine, are currently incompatible with RNA recovery. Therefore, despite the fact that our sampling of HVC cells of the replaceable kind included only those that could be backfilled and were, therefore, presumably already part of a functioning circuit, our gene expression results for these cells probably came from cells of a span of ages. Some cells might have been born 1 month ago; others may have been born many months earlier, and their life expectancies may have varied as well. Yet we see across these cells a dramatically lower mean level of *UCHL1* expression. Similarly, the up-regulation of *UCHL1* with singing that we saw in the RA-projecting neurons was robust and measurable, although we do not know whether the life expectancy of all these cells had been prolonged by singing (14). These same caveats apply to our mouse material and even more so, because the selection of cells to harvest was not determined by backfills but rather by the affiliation of a cell with a particular layer.

Implications of Low Levels of *UCHL1* in Brain Regions Undergoing Neuronal Replacement. Our results show that, in parts of the adult brain where neuronal replacement occurs (HVC, hippocampus, olfactory bulb), *UCHL1* expression was at its lowest in the

replaceable neurons. Why might replaceable neurons from these disparate brain regions of birds and mammals share depressed levels of *UCHL1*? One possibility is that *UCHL1* expression has to do with neuron size. For example, in our three comparisons, the replaceable neurons were, in each case, the smaller of the two cell types compared. We have not sampled enough cells of various sizes to know whether this correlation holds further, but it is possible that constitutive *UCHL1* expression levels are related to, for example, a neuron's total cytoplasmic volume. Another possibility is that the average age of the neurons matters. Nonreplaceable neurons will, by definition, have a greater mean age than replaceable ones, and *UCHL1* expression levels may increase with cell age, as has been suggested for UCHL1 protein in pituitary neurons (34). There are ways of teasing apart the age variable, but we have not yet done so. The third possibility, and the one toward which we incline, is that relatively low levels of UCHL1 expression reflect neuronal life expectancy. UCHL1, as part of the ubiquitin–proteasome system necessary for protein degradation, has been implicated in the death of neurons in neurodegenerative diseases, such as Parkinson's, Alzheimer's, and Huntington's (35–38). A mouse mutant for *UCHL1* also shows axonal loss and cell death (39). In the human disease states, *UCHL1* levels are low (36) or its function is compromised (26, 37); in the mutant mouse, there is a UCHL1 loss-of-function mutation (40). The shared theme of impending neuronal death in spontaneous neuronal replacement and in neurodegeneration may explain the association of these two events with low *UCHL1* expression levels. We do not know, however, whether in both scenarios low *UCHL1* function would have similar consequences for protein turnover or whether low levels of *UCHL1* function would affect other cell functions (41, 42). However, the magnitude of down-regulation of protein degradation need not be large to affect a cell's survival. In one study (43), an average 38% reduction in proteasome function was found in the substantia nigra of patients with Parkinson's disease. These results suggest that dipping below a threshold level of proteasome function may lead to neuronal death. A similar threshold may exist for *UCHL1* expression levels in the case of spontaneous neuronal death, although we do not yet have information on UCHL1 protein levels in replaceable neurons. It will be important to understand why different types of neurons express different amounts of *UCHL1* and whether low levels indicate, necessarily, impending neuronal death. Studies addressing why different kinds of permanent neurons express this gene at widely disparate levels may also contribute to our understanding of the function of UCHL1 protein. It would be ironic if the shortfall in a same gene brokered the path to brain disease or rejuvenation.

We thank Dr. Kan Yang and the Strang Cancer Prevention Center at The Rockefeller University for access to the Pixcell IIe laser capture microscope; Terry Gaasterland and XiuJie Wang for bioinformatics assistance; Rudy Spangler for advice on TaqMan; Philip Iredale, Frank Menniti, and Leopoldo Petreanu for helpful discussions; Sattie Haripal, Laurel Martin-Harris, and the Gene Array Resource Center at The Rockefeller University for outstanding technical assistance throughout these experiments; Drs. Bruce McEwen and Arturo Alvarez-Buylla for critical reading of the manuscript; and Daun Jackson, Sharon Sepe, and Helen Ecklund for excellent bird care. This work was supported by a postdoctoral fellowship from Pfizer Global Research and Development (to A.J.L.), by National Institute of Mental Health Grant MH18343 (to F.N.), and by the generosity of Mr. Howard Phipps and the Herbert and Nell Singer Foundation.

1. Nottebohm, F. (2002) *Brain Res. Bull.* **57,** 737–749.
2. Kirn, J. & Nottebohm, F. (1993) *J. Neurosci.* **13,** 1654–1663.
3. Scharff, C., Kirn, J., Grossman, M., Macklis, J. D. & Nottebohm, F. (2000) *Neuron* **25,** 481–492.
4. Gould, E., Vail, N., Wagers, M. & Gross, C. G. (2001) *Proc. Natl. Acad. Sci. USA* **98,** 10910–10917.
5. Kaplan, M. S. & Hinds, J. W. (1977) *Science* **197,** 1092–1094. .
6. Petreanu, L. & Alvarez-Buylla, A. (2002) *J. Neurosci.* **22,** 6106–6113.
7. Goldman, S. A. & Nottebohm, F. (1983) *Proc. Natl. Acad. Sci. USA* **80,** 2390–2394.
8. Alvarez-Buylla, A., Seri, B. & Doetsch, F. (2002) *Brain Res. Bull.* **57,** 751–758.
9. Alvarez-Buylla, A. & Nottebohm, F. (1988) *Nature* **335,** 353–354.
10. Lois, C. & Alvarez-Buylla, A. (1994) *Science* **264,** 1145–1148.
11. Paton, J. A. & Nottebohm, F. (1984) *Science* **225,** 1046–1048.
12. van Praag, H., Schinder, A. F., Christie, B. R., Toni, N., Palmer, T. D. & Gage, F. H. (2002) *Nature* **415,** 1030–1034.
13. Kirn, J. R., Fishman, Y., Sasportas, K., Alvarez-Buylla, A. & Nottebohm, F. (1999) *J. Comp. Neurol.* **411,** 487–494.
14. Li, X. C., Jarvis, E. D., Alvarez-Borda, B., Lim, D. A. & Nottebohm, F. (2000) *Proc. Natl. Acad. Sci. USA* **97,** 8584–8589.
15. Gould, E., Beylin, A., Tanapat, P., Reeves, A. & Shors, T. J. (1999) *Nat. Neurosci.* **2,** 260–265.
16. Alvarez-Borda, B., Haripal, B. & Nottebohm, F. (2004) *Proc. Natl. Acad. Sci. USA* **101,** 3957–3961.
17. Markakis, E. A. & Gage, F. H. (1999) *J. Comp. Neurol.* **406,** 449–460.
18. Wang, S., Scott, B. W. & Wojtowicz, J. M. (2000) *J. Neurobiol.* **42,** 248–257.
19. Kronenberg, G., Reuter, K., Steiner, B., Brandt, M. D., Jessberger, S., Yamaguchi, M. & Kempermann, G. (2003) *J. Comp. Neurol.* **467,** 455–463.
20. Alvarez-Borda, B. & Nottebohm, F. (2002) *J. Neurosci.* **22,** 8684–8690.
21. Wild, J. M., Williams, M. N., Howie, G. J. & Mooney, R. (2005) *J. Comp. Neurol.* **483,** 76–90.
22. Alvarez-Buylla, A., Kirn, J. & Nottebohm, F. (1990) *Science* **249,** 1444–1446.
23. Van Gelder, R. N., von Zastrow, M. E., Yool, A., Dement, W. C., Barchas, J. D. & Eberwine, J. H. (1990) *Proc. Natl. Acad. Sci. USA* **87,** 1663–1667.
24. Bustin, S. A. (2000) *J. Mol. Endocrin.* **25,** 169–193.
25. Lorkowski, S. & Cullen, P. (2003) *Analysing Gene Expression* (Wiley, Weinheim, Germany).
26. McNaught, K. S., Olanow, C. W., Halliwell, B., Isacson, O. & Jenner, P. (2001) *Nat. Rev. Neurosci.* **2,** 589–594.
27. Osaka, H., Wang, Y.-L., Takada, K., Takizawa, S., Setsuie, R., Li, H., Sato, Y., Nishikawa, K., Sun, Y.-J., Sakurai, M., *et al.* (2003) *Hum. Mol. Gen.* **12,** 1945–1958.
28. Wilkinson, K. D., Lee, K., Deshpande, S., Duerksen-Hughes, P., Boss, J. M. & Pohl, J. (1989) *Science* **246,** 670–673.
29. Jackson, P., Thomson, V. M. & Thompson, R. J. (1985) *J. Neurochem.* **45,** 185–190.
30. Kempermann, G., Gast, D., Kronenberg, G., Yamaguchi, M. & Gage, F. (2003) *Development (Cambridge, U.K.)* **130,** 391–399.
31. Carleton, A., Petreanu, L. T., Lansford, R., Alvarez-Buylla, A. & Lledo, P.-M. (2003) *Nat. Neurosci.* **6,** 507–518.
32. Hegde, A. N., Inokuchi, K., Pei, W., Casadio, A., Ghirardi, M., Chain, D. G., Martin, K. C., Kandel, E. R. & Schwartz, J. H. (1997) *Cell* **89,** 115–126.
33. Chang, C., Chang, A. Y. & Chan, S. H. (2004) *Shock* **22,** 575–581.
34. Marzban, G., Grillari, J., Reisinger, E., Hemetsberger, T., Grabherr, R. & Katinger, H. (2002) *Exp. Neurol.* **37,** 1451–1460.
35. Dawson, T. M. & Dawson, V. L. (2003) *Science* **302,** 819–822.
36. Choi, J., Levey, A. I., Weintraub, S. T., Rees, H. D., Gearing, M., Chin, L.-S. & Li, L. (2004) *J. Biol. Chem.* **279,** 13256–13264.
37. Giasson, B. I. & Lee, V. M.-Y. (2003) *Cell* **114,** 1–8.
38. Naze, P., Vuillaume, I., Destee, A., Pasquier, F. & Sablonniere, B. (2002) *Neurosci. Lett.* **328,** 1–4.
39. Mukoyama, M., Yamazaki, K., Kikuchi, T. & Tomita, T. (1989) *Acta Neuropathol.* **79,** 294–299.
40. Saigoh, K., Wang, Y.-L., Suh, J.-G., Yamanishi, T., Sakai, Y., Kiyosawa, H., Harada, T., Ichihara, N., Wakana, S., Kikuchi, T. & Wada, K. (1999) *Nat. Gen.* **23,** 47–51.
41. Chung, C. H. & Baek, S. H. (1999) *Biochem. Biophys. Res. Commun.* **266,** 633–640.
42. Liu, Y., Fallon, L., Lashuel, H. A., Liu, Z. & Lansbury, P. T., Jr. (2002) *Cell* **111,** 209–218.
43. McNaught, K. S. & Jenner, P. (2001) *Neurosci. Lett.* **297,** 191–194.